VIII International Conference on Computational Methods for Coupled Problems in Science and Engineering
COUPLED PROBLEMS 2019
E. Oñate, M. Papadrakakis and B. Schrefler (Eds)

SOIL-STRUCTURE INTERACTION SIMULATIONS TAKING INTO ACCOUNT THE TRANSIENT PROPAGATION OF SEISMIC WAVES

Marco Schauer*, Francesca Taddei+ and Gustavo A. Ríos Rodriguez†

* Institut für Statik
Technische Universität Braunschweig
Beethovenstraße 51, 38106 Braunschweig, Germany
e-mail: m.schauer@tu-braunschweig.de, web page: https://www.tu-braunschweig.de/statik

+ Chair of Structural Mechanics
Technical University of Munich
Arcisstr. 21, 80333 Munich, Germany
e-mail: francesca.taddei@tum.de, web page: https://www.bm.bgu.tum.de

†Centro de Investigación de Métodos Computacionales
CIMEC (UNL - CONICET)
Predio CONICET-Santa Fe, Colectora RN 168, El Pozo, 3000 Santa Fe, Argentina
e-mail: gusadrr@yahoo.com.ar - web page: https://cimec.org.ar

Key words: Soil-Structure Interaction, Finite Element Method, Scaled Boundary Finite Element Method, Wave propagation, Earthquake, Time Domain Analysis

Abstract. In this contribution we present a strategy to investigate the vibrations of buildings subjected to a transient seismic excitation, including the soil-structure interaction. The proposed simulation method can be helpful during the design of earthquake-resistant structures in seismic active areas as well as for the design of vibration reduction measures for buildings subjected to surrounding emissions like vibrations induced by traffic or machine foundations. The structures and their foundation as well as parts of the soil are modeled by Finite Element Method (FEM). The far field is idealized as an infinite half-space and modeled with the Scaled Boundary Finite Element Method (SBFEM). Both methods are coupled at the common interface. This approach fulfills exactly the Sommerfeld radiation condition. The seismic excitation is idealized as a plane wave propagating toward the structure with an arbitrary angle with respect to the soil surface. The 3D seismic wave field, caused by the wave passage at the near field boundary, is transformed into boundary tractions, which are then applied at the interface between the near and far fields. We present an application of the proposed method for a group of three buildings, which interact with each other through the soil during the propagation of the transient seismic waves. Although not shown here, the proposed method can handle nonlinear material properties assigned to any element of FEM part.

1 INTRODUCTION

During a seismic event, the excited buildings interact with the soil and with each other through the soil, leading to a complex highly scattered oscillation response. A realistic representation of the seismic soil-structure interaction (SSI) requires a high computational workload, especially when computing the transient nonlinear response of the coupled soil-structures system. The main questions of seismic SSI investigations are: 1) How is the seismic excitation estimated and applied to the SSI system? 2) How is the seismic response of one or more buildings influenced by the interaction with the flexible soil?

The two questions are intrinsically related because the propagation of seismic waves from a source and the response of the near field underneath the structure are both governed by the same mathematical description, the Lamé equations, and therefore cannot be solved independently.

However, the most common approach to answer the two questions is to treat them separately. Indeed, the seismic SSI can be seen as multiresolution problem: the far-field scale for the simulation of the propagation of seismic waves in the free field and the near-field scale for the simulation of the SSI system. This assumption is at the heart of the Domain Reduction Method (DRM) [21, 7, 5]. In the DRM, the problem is solved in two steps: in a first step, the displacement field of the soil due to a far field source is computed for a specific region at the boundary of the near field; in a second step, equivalent seismic loads are derived from this displacement and applied as input to a small-scale model, which includes the near field and the buildings.

At the far-field scale, the free field motions caused by a seismic event are mainly characterized by a low-frequency content, because short-wavelength waves are dissipated during the propagation towards the structure through large distances. Analytical solutions for the Lamé equations only exist for very idealized soil profiles and, therefore, numerical approaches are preferred. Currently, the most established method for computing the large-scale three-dimensional 3D far field is the Finite Element Method (FEM) with several extensions such as high order elements [17], spectral elements [6] and discontinuous Galerkin method [8]. These models deliver the seismic input at a certain near field surface (either at the SSI interface or at the near field boundary). Depending on the size of the considered far field, in many cases the maximum considered frequency in the simulation is between 2 and 5 Hz, to keep the element number affordable.

Once the first step is performed, the seismic excitation is applied to the small-scale model for the near field scenario, which couples the buildings with each other through the soil and, at the same time, satisfy the radiation conditions. At the near-field scale, a higher maximum frequency is necessary and, therefore, a much finer mesh is required. One common option for the modelling of the infinite soil in the small-scale model is the FEM extended with transmitting boundaries (TB) [1]. These are special elements at the boundaries of the FEM domain: paraxial boundaries, perfectly-matched layers (PML), infinite elements or scaled boundary finite elements (SBFEM). The FEM can account for

nonlinearities in the structure as well as in the soil near field and can be solved using direct time integration methods such as central difference method or Newmark method. The soil's far field is assumed to remain linear. An alternative to the transmitting boundaries, the boundary element method [18], the discrete wavenumber method [10] and the integral transform method [3] have been popular for problems with relatively simple geometry and geological conditions. These are based on the fundamental solution of the Lamé equations and can be coupled to the FEM using the substructure approach, but their application is limited to linear cases and homogenous or horizontally layered soils.

One drawback of the DRM is that the type of earthquake source of the seismic event must be known in detail and this is not always possible. Moreover, two different models (with different scales) need to be generated and run. In this contribution we propose an

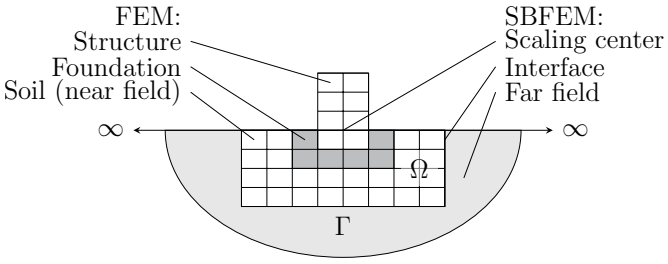

Figure 1: Problem definition [14].

efficient 3D method for the simulation of the seismic SSI. The substructuring method is used, where the problem is subdivided into two sub-systems (cf. figure 1). The near field, which contains the structure and its foundation as well as parts of the soil, is modeled by FEM. The far field of the infinite half-space is discretized by the SBFEM. Both sub-systems are coupled at the common interface of FEM and SBFEM Γ [20].

We assume that the buildings are at great distance from the sources and the wavefront can be considered plane. In this case the seismic excitation is simulated as a transient plane wave that propagates through the far field at a constant speed inclined with a certain angle with respect to the free field surface. The accelerations due to the passing plane wave are computed for the free field (without buildings) at the outer nodes of the near field boundary and are translated into equivalent seismic loads. These loads are used in the full seismic SSI system to transfer the plane wave to the near field. The main assumptions are that the seismic input is not strongly affected by the presence of the buildings and that the seismic input reaches the near field as a plane wave.

2 FEM-SBFEM COUPLING

The FEM-SBFEM coupling is described briefly, more information about the theoretical background and its efficient implementation can be found in Schauer et al. [11, 13]. The

equation of motion is given by

$$\begin{bmatrix} \boldsymbol{M}_{\Omega\Omega} & \boldsymbol{M}_{\Omega\Gamma} \\ \boldsymbol{M}_{\Gamma\Omega} & \boldsymbol{M}_{\Gamma\Gamma} \end{bmatrix} \ddot{\boldsymbol{u}} + \begin{bmatrix} \boldsymbol{C}_{\Omega\Omega} & \boldsymbol{C}_{\Omega\Gamma} \\ \boldsymbol{C}_{\Gamma\Omega} & \boldsymbol{C}_{\Gamma\Gamma} \end{bmatrix} \dot{\boldsymbol{u}} + \begin{bmatrix} \boldsymbol{K}_{\Omega\Omega} & \boldsymbol{K}_{\Omega\Gamma} \\ \boldsymbol{K}_{\Gamma\Omega} & \boldsymbol{K}_{\Gamma\Gamma} \end{bmatrix} \boldsymbol{u} = \begin{bmatrix} \boldsymbol{p}_{\Omega\Omega} \\ \boldsymbol{p}_{\Gamma\Gamma} \end{bmatrix} + \begin{bmatrix} \boldsymbol{0} \\ \boldsymbol{p}_b \end{bmatrix}, \quad (1)$$

which is divided up, so that $\Omega\Omega$ contains all near field nodes and $\Gamma\Gamma$ contains all far field nodes. $\Omega\Gamma$ and $\Gamma\Omega$ represent the coupling nodes of near field and far field. $\boldsymbol{M}$, $\boldsymbol{C}$ and $\boldsymbol{K}$ represent mass, damping and stiffness matrix and the vectors $\boldsymbol{u}$, $\dot{\boldsymbol{u}}$ and $\ddot{\boldsymbol{u}}$ denote displacement, velocity and acceleration. The vector $\boldsymbol{p}$ represents the applied nodal forces. $\boldsymbol{p}_b$ contains the influence of the infinite half-space, which is described by SBFEM. The interacting forces at the interface Γ are given by the vector

$$\boldsymbol{p}_b(t_n) = \gamma \Delta t \boldsymbol{M}_0^{\infty} \ddot{\boldsymbol{u}}_n + \sum_{j=1}^{n-1} \boldsymbol{M}_{n-j}^{\infty} \left(\dot{\boldsymbol{u}}_j - \dot{\boldsymbol{u}}_{j-1} \right). \quad (2)$$

Here γ and Δt are parameters introduced by the time integration scheme. The unit acceleration impulse matrices or influence matrices $\boldsymbol{M}^{\infty}$ are assumed to be constant within one time step. This matrices are computed in a pre-process applying model reduction techniques to reduce numerical effort [14]. Inserting equation (2) into equation (1) yields a direct and bidirectional coupled FEM-SBFEM formulation

$$\begin{aligned} &\begin{bmatrix} \boldsymbol{M}_{\Omega\Omega} & \boldsymbol{M}_{\Omega\Gamma} \\ \boldsymbol{M}_{\Gamma\Omega} & \boldsymbol{M}_{\Gamma\Gamma} + \gamma \Delta t \boldsymbol{M}_0^{\infty} \end{bmatrix} \ddot{\boldsymbol{u}} + \begin{bmatrix} \boldsymbol{C}_{\Omega\Omega} & \boldsymbol{C}_{\Omega\Gamma} \\ \boldsymbol{C}_{\Gamma\Omega} & \boldsymbol{C}_{\Gamma\Gamma} \end{bmatrix} \dot{\boldsymbol{u}} + \begin{bmatrix} \boldsymbol{K}_{\Omega\Omega} & \boldsymbol{K}_{\Omega\Gamma} \\ \boldsymbol{K}_{\Gamma\Omega} & \boldsymbol{K}_{\Gamma\Gamma} \end{bmatrix} \boldsymbol{u} \\ &\qquad = \begin{bmatrix} \boldsymbol{p}_{\Omega\Omega} \\ \boldsymbol{p}_{\Gamma\Gamma} - \sum_{j=1}^{n-1} \boldsymbol{M}_{n-j}^{\infty} \left(\dot{\boldsymbol{u}}_j - \dot{\boldsymbol{u}}_{j-1} \right) \end{bmatrix}. \end{aligned} \quad (3)$$

The damping matrix is a combination of weighted mass matrix and stiffness matrix according to the Rayleigh representation

$$\boldsymbol{C} = c_m \boldsymbol{M} + c_k \boldsymbol{K}. \quad (4)$$

The calculation in the time domain is performed by executing the generalized-α time integration scheme [2].

3 TRANSIENT WAVES

To simulate transient waves through the far field we consider: at first seismic wave propagates through the far field at a constant speed inclined with a certain angle, as shown in figure 2 and secondly the seismic forces as external loads contained in the vector $\boldsymbol{p}_{\Gamma\Gamma}$ in equation (3). This approach is an efficient approximation to avoid the computation of the interaction forces at the interface Γ, which would require the relative quantities in equation (3) in place of $\dot{\boldsymbol{u}}_j$.

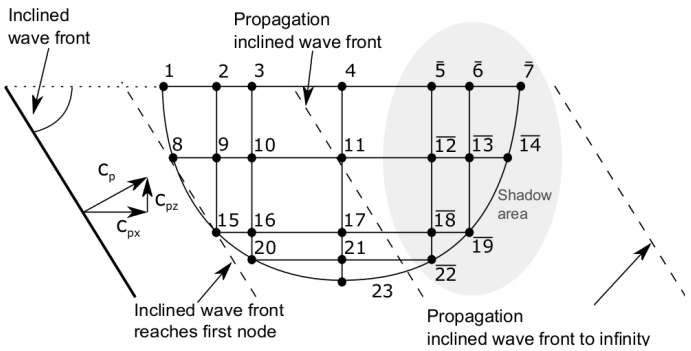

Figure 2: Simplified sketch of propagation of inclined wave fronts as represented in the numerical model [15].

The movement of the particle of the wave front can be governed by an arbitrary time-dependent accelerogram $a(t)$. When the wave front reaches the near field the nodes at the interface Γ are accelerated at different time steps, depending on the nodes position, e.g. figure 2. For the computation of the boundary tractions, only the outer nodes are considered, so that the wave front is transferred homogeneously to the near field. The nodes which are located in the shadowed areas are not loaded, to avoid inhomogeneous effects due to waves travelling in opposite direction w.r.t the wavefront. The loads are computed by $\boldsymbol{p}_{\Gamma\Gamma} = \boldsymbol{M}\mathbf{1}a(t)$, where $\boldsymbol{M}$ is the mass matrix e.g. equation (1). $\mathbf{1}$ is a vector that contains ones at the degrees of freedom accelerated by the wave front and $a(t)$ contains the scalar information of nodal acceleration.

4 APPLICATION

Figure 3 shows the considered near-field as well as three buildings, to which the seismic waves are applied. The seismic wavefront is vertical and it propagates in horizontal direction (its ray is the x-axis) with constant speed equal to c_p and the particles move in horizontal direction. The transient wavefront accelerates the outer nodes of the near field boundary at different time steps and the resulting boundary tractions at the interface between near and far field generate a spatially scattered seismic field at the soil surface. Even if the plane wavefront gives an input in x-direction where all the particles in the vertical plane are in-phase, the resulting ground motions at the surface for the SSI system have non-zero components also in z- and y-direction. This is the consequence of both the combination of body and surface waves and the scattering effect of the oscillating buildings (asymmetric w.r.t. the x-axis) on the free field motions.

The domain of interest is a half sphere with a radius of 100 [m]. The discretization is done by FEM as described before and the finite element mesh consists of 20989 nodes, 18744 elements and so 62967 degrees of freedom. To gain results in a reasonable time, mapping methods are utilized to transfer state variables like velocity, acceleration and forces between FEM and SBFEM discretization. This has the advantage that non-matching

meshes in space can be used and the computational effort is reduced significantly [16]. Here, the time discretization is the same in FEM and SBFEM. While the interface (the surface of the FEM domain) has 2370 nodes, 2316 elements and 7110 degrees of freedom the SBFEM domain comes out with only 287 nodes, 229 elements and 861 degrees of freedom.

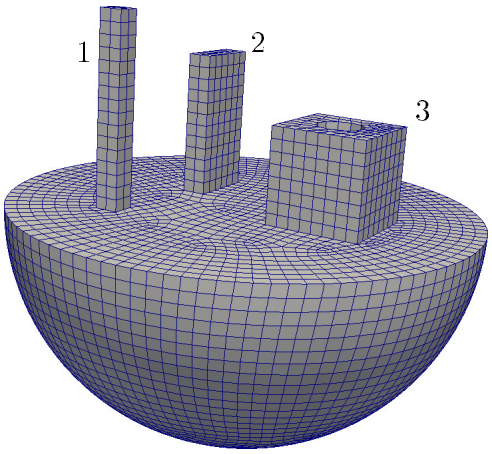

Figure 3: Views of the near field with three buildings [12].

The buildings in this example are designed as solid blocks and are therefore very much simplified, they serve only for illustrative purposes. The buildings geometric dimensions like width, depth and height as well as the chosen material parameters like Young's modulus, Poisson ratio and density are summarized in table 1. The cylindrical opening inside the third building has a radius of 10 [m]. Young's modulus, Poisson ratio, and density of the soil are $100 \cdot 10^6$ [Nm^{-2}], 0.30 [-], and 2200 [kgm^{-3}], respectively. This leads to a p-wave velocity c_p of 247.36 [ms^{-1}].

Table 1: Summary of buildings geometric dimensions and material characteristics.

	width [m]	depth [m]	height [m]	Young's modulus [Nm^{-2}]	Poisson [-]	density [kgm^{-3}]
building 1	5	5	80	$200 \cdot 10^6$	0.30	1000
building 2	30	5	60	$10 \cdot 10^6$	0.15	500
building 3	40	40	40	$10 \cdot 10^6$	0.15	450

In order to set up the damping coefficients of the Rayleigh damping (see equation (4)) a modal analysis is conducted. Therefore the eigenvalue problem

$$\det \left| \boldsymbol{M}\lambda^2 + \boldsymbol{K} \right| \boldsymbol{x} = \boldsymbol{0} \tag{5}$$

is solved to compute the unknown eigenvalues λ and the corresponding natural frequencies ω. Some vibration modes are illustrated in table 2. Table 3 lists a specification of the vibration modes for natural frequencies within the range of 0.2 to 3.0 $[s^{-1}]$. Higher natural frequencies are a combination of modes and can not be clearly assigned.

Table 2: Illustration of some modes. The mode description is given in table 3.

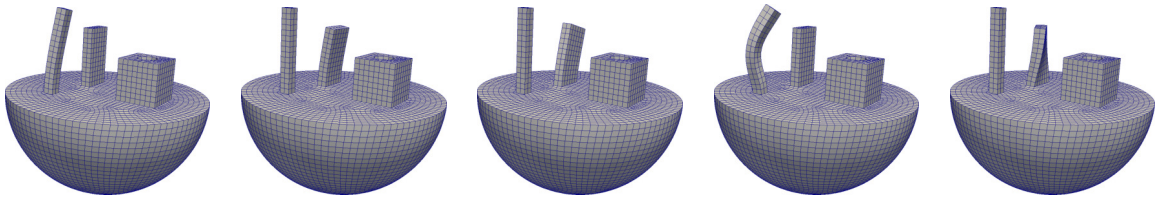

0.2468 $[s^{-1}]$ 0.4134 $[s^{-1}]$ 1.0300 $[s^{-1}]$ 1.4680 $[s^{-1}]$ 1.5321 $[s^{-1}]$

Table 3: Natural frequencies and corresponding modes within the range of 0.2 to 3.0 $[s^{-1}]$.

Natural freq. ω $[s^{-1}]$	Frequency f [Hz]	Period T [s]	Mode
0.2468	1.5507	0.6449	building 1 first bending mode x-direction
0.2469	1.5513	0.6446	building 1 first bending mode y-direction
0.4134	2.5975	0.3850	building 2 first bending mode x-direction
1.0300	6.4717	0.1545	building 2 first bending mode y-direction
1.4680	9.2237	0.1084	building 1 second bending mode x-direction
1.4684	9.2262	0.1084	building 1 second bending mode y-direction
1.5321	9.6265	0.1039	building 2 first torsion mode
1.9282	12.1152	0.0825	building 2 second bending mode x-direction
2.2632	14.2201	0.0703	building 1 third bending mode x-direction
2.2701	14.2635	0.0701	building 2 third bending mode x-direction
2.3763	14.9307	0.0670	building 1 first tension mode
2.9115	18.2935	0.0547	and higher are combined modes, not clearly assignable

To determine c_m and c_k we chose from building 1 and 2 the natural frequencies of the first bending modes $\omega_1 = 0.2468$ $[s^{-1}]$ and $\omega_3 = 0.4134$ $[s^{-1}]$. The damping ratio ς is set to 5% since we assume the buildings to be reinforced concrete structures. This leads to the Rayleigh damping coefficients [9]

$$c_m = \varsigma \frac{2\omega_1\omega_3}{\omega_1 + \omega_3} = 0.015 \text{ [s]} \quad \text{and} \quad c_k = \varsigma \frac{2}{\omega_1 + \omega_3} = 0.151 \text{ } [s^{-1}] \quad . \tag{6}$$

As described in section 3 seismic loads are considered in $\boldsymbol{p}_{\Gamma\Gamma}$. Here the numerical analysis is conducted with a strong earthquake event. Figure 4 shows the acceleration-time-plot of the Kobe, Japan earthquake in 1995. It has a moment magnitude scale of $M_w = 7.2$. The major acceleration takes place within the range 7 to 15 seconds, which means a time slot of 8 seconds.

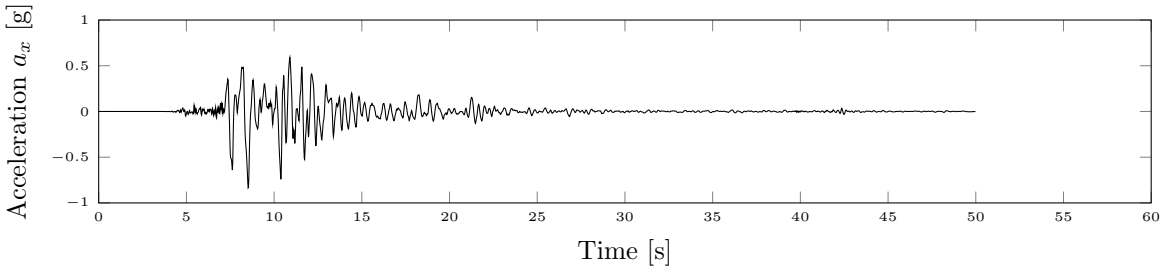

Figure 4: Earthquake acceleration Kobe, Japan, 1995.

Since the acceleration-time-plot of Kobe earthquake has a duration of 50 [s] and the p-wave needs approximately 1 [s] to run through the domain of interest, 60 [s] of simulation time are conducted. The time step length in both domains FEM and SBFEM is chosen to $\Delta t = 1.0 \cdot 10^{-3}$ $[s]$, so that $60 \cdot 10^3$ time steps are evaluated. The Generalized-α Methods time integration parameter is set to $\rho^{\infty} = 0.8$.

To discuss the solution representative nodes are chosen, as shown in table 4a. For each building one node at its foundation as well as one node at its top is observed. For these observed nodes the nodal displacement for each spatial direction is shown in tables 4b-d. In the upper part of the pictures the results at the buildings top and in the lower part the results at the interface between ground and building are presented. The excitation reaches the buildings at different time steps, depending on their position with respect to the propagation direction, which points from the negative to the positive x-axis. First, the seismic load affects node 424, then node 115, and lastly node 5789. Thus, the simulation shows a correct sequence of events. Even though the seismic excitation is computed independently from the presence of the buildings, the SSI interaction has an influence on the motion of the ground surface. This can be seen in table 5, which shows the Fourier transformed displacements of the Kobe earthquake as well as the buildings top and base displacements: the displacements at the ground level of the buildings have modified frequency content w.r.t. the input. The FEM-SBFEM coupling allows to simulate the passage of waves through the near field without being reflected at its boundary and therefore fulfilling the radiation condition.

Table 4: Components of the displacement field versus time, at the base and top nodes of the buildings.

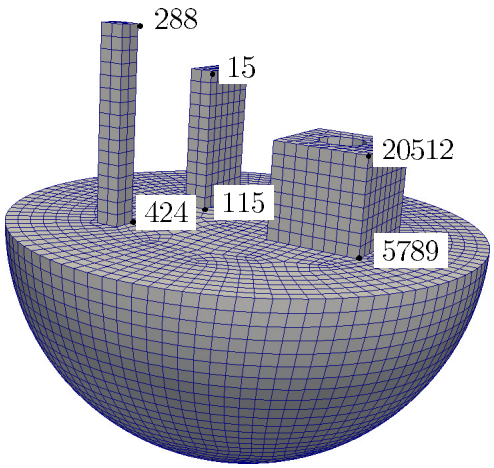

a) Observed nodes.

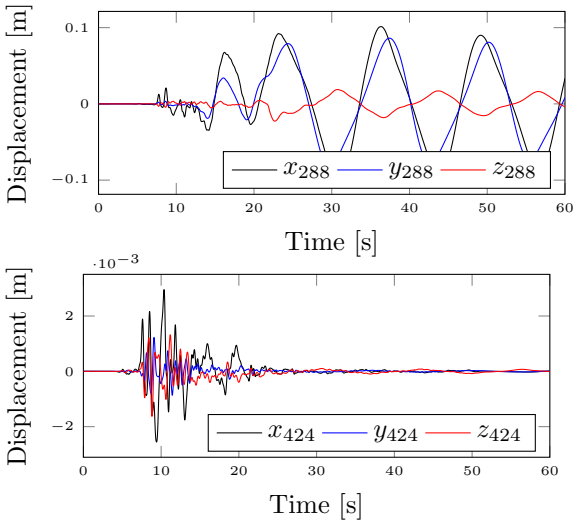

b) Building 1 nodes 424 and 288.

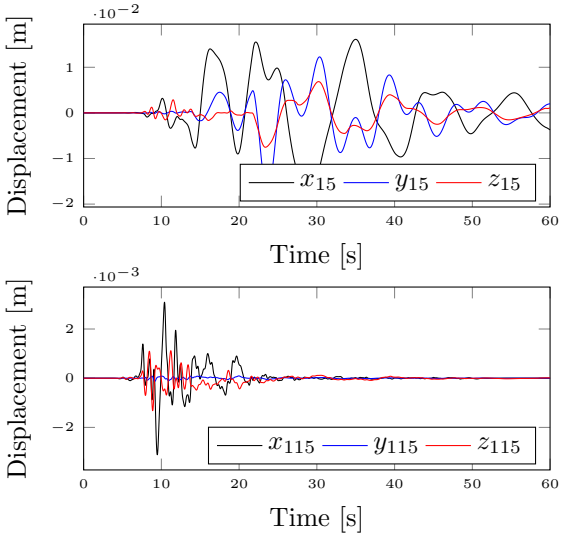

c) Building 2 nodes 115 and 15.

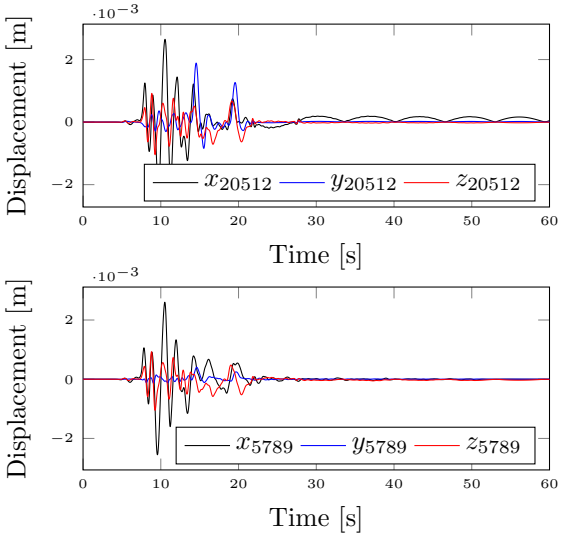

d) Building 3 nodes 5789 and 20512.

5 CONCLUSION

The proposed approach allows to simulate one or more buildings coupled to the underlying soil subjected to 3D plane ground-born seismic wave fronts, including the SSI effects. Such simulations can be used to determine maximum displacements, velocities, accelerations, stress and strains of buildings or other constructions, which can be used

Table 5: Spectra of the displacements in x-direction for the input and the outputs.

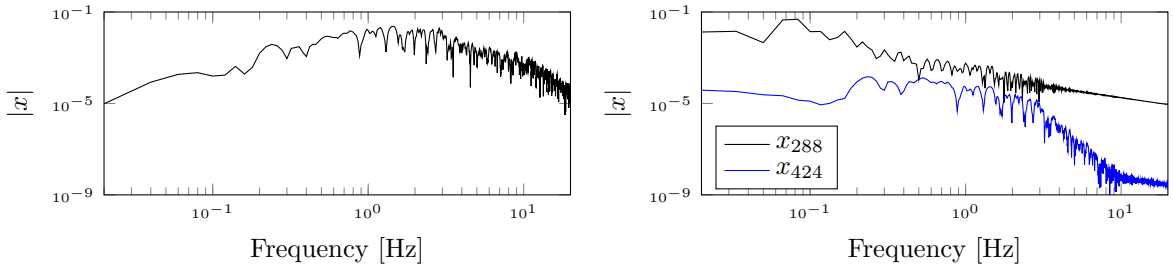

a) Input displacements of the wavefront.

b) Output displacements of building 1.

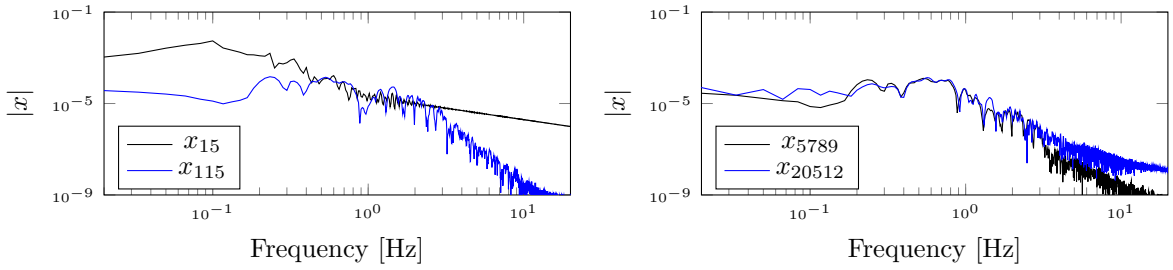

c) Output displacements of building 2.

d) Output displacements of building 3.

for seismic design verifications or for the improvement of the usability/comfort. It is assumed that the buildings are a large distance form the excitation source, where the wave front becomes plane and the ray has a certain inclination w.r.t. the soil surface. The FEM/SBFEM coupling combined with the approximated methodology for the simulation of transient ground-born wave front provides good physical insights into the complex problem with reasonable results, a practical implementation of the input for the seismic excitation and a limited calculation time. For future improvement, the FEM/SBFEM coupling will be used to investigate nonlinear processes in the near field due to strong earthquakes.

REFERENCES

[1] Astley, R. J.: *Infinite elements for wave problems: a review of current formulations and an assessment of accuracy*, International Journal for Numerical Methods in Engineering , 49(7), 951-976, 2000.

[2] Chung, J.; et al.: *A Time Integration Algorithm for Structural Dynamics with Improved Numerical Dissipation: The Generalized-α Method*, Journal of Applied Mechanics, 60, 372–375, 1993.

[3] Freisinger, J.; Müller, G.: *Modellierung eines Halbraums mit sphärischem oder zylin-*

derförmigem Hohlraum für dreidimensionale Boden-Bauwerk-Interaktion, Forschung im Ingenieurwesen, 89(1), 1-12, 2019.

[4] Isbiliroglu, Y.; et al.: *Coupled soil-structure interaction effects of building clusters during earthquakes*, Earthquake Spectra, 31(1), 463-500, 2017.

[5] Jeremic, B.; et al.: *Time domain simulation of soil-foundation-structure interaction in non-uniform soils*, Earthquake Engineering & Structural Dynamics, 38(5), 699-718, 2009.

[6] Khan, S.; et al.: *Impact of mesh and DEM resolutions in SEM simulation of 3D seismic response*, Bulletin of the Seismological Society of America, 107(5), 2151-2159, 2017.

[7] Kontoe, S.; et al.: *The domain reduction method for dynamic coupled consolidation problems in geotechnical engineering*, International journal for numerical and analytical methods in geomechanics, 32(6), 659-680, 2008.

[8] Mazzieri, I.; et al.: *SPEED: SPectral Elements in Elastodynamics with Discontinuous Galerkin: a non-conforming approach for 3D multi-scale problems*, International Journal for Numerical Methods in Engineering, 95(12), 991-1010, 2013.

[9] Petersen, C.: *Dynamik der Baukonstruktionen* ,Vieweg & Sohn Verlagsgesellschaft mbH, Braunschweig/Wiesbaden, 2000.

[10] Restrepo, D.; et al: *SH wave number Green's function for a layered, elastic half-space. Part I: Theory and dynamic canyon response by the discrete wave number boundary element method*, Pure and Applied Geophysics, 171(9), 2185-2198, 2014.

[11] Schauer, M.; Roman, E.J.; Quintana-Ortí, E.S.; Langer, S.: Parallel Computation of 3-D Soil-Structure Interaction in Time Domain with a Coupled FEM/SBFEM Approach, Journal of Scientific Computing, Vol. 52, pp. 446–467, 2012.

[12] Schauer M.; *Ein effizienter gekoppelter FEM-SBFEM Ansatz zur Analyse von Boden-Bauwerk-Interaktionen im Zeitbereich* Dissertation, Fakultät Architektur, Bauingenieurwesen und Umweltwissenschaften,Technischen Universität Carolo-Wilhelmina zu Braunschweig, 2014.

[13] Schauer, M.; Langer, S.: *Implementation of an Efficient Coupled FEM-SBFEM Approach for Soil-Structure-Interaction Analysis* in B.A. Schrefler; E. Oñate; M. Papadrakakis (Ed.) Proceedings of the VI International Conference on Coupled Problems in Science and Engineering, 370–381, 2015.

[14] Schauer, M.: *On the influence of far-field model reduction techniques using a coupled FEM-SBFEM approach in time domain*, Journal of Mathematical Sciences and Modeling, 1 93–104, 2018.

[15] Schauer M.; Taddei, F. and Ríos Rodriguez G. *Seismic Transient Simulation of an Operating Wind Turbine Considering the Soil-Structure Interaction*, RASD, 2019.

[16] Schauer M. and Ríos Rodriguez G. *A Coupled FEM-SBFEM Approach for Soil-Structure-Interaction Analysis Using Non-Matching Meshes at the Near-Field Far-Field Interface*, Soil Dynamics and Earthquake Engineering, Accepted Date : 27-Jan-2019.

[17] Semblat, J.-F.; et al.:*Seismic-wave propagation in alluvial basins and influence of site-city interaction*, Bulletin of the Seismological Society of America, 98(6), 2665-2678, 2008.

[18] Taddei, F., Meskouris, K.: *Seismic analysis of onshore wind turbine including soil-structure interaction effects*, Seismic Design of Industrial Facilities, Springer Vieweg, Wiesbaden, 511-522, 2014.

[19] Wolf J. and Song C. *Finite-Element Modelling of Unbounded Media*. John Wiley & Sons, Chichester, 1996.

[20] Wolf J. *The Scaled Boundary Finite Element Method* John Wiley & Sons, Chichester, 2003.

[21] Yoshimura, C.; et al.: *Domain reduction method for three-dimensional earthquake modeling in localized regions, part II: Verification and applications*, Bulletin of the Seismological Society of America, 93(2), 825-841, 2003.

[22] Zienkiewicz, O.C. and Taylor, R.L. *The finite element method.* McGraw Hill, Vol. II., 1991.